ELSEVIER

Chemical Engineering Journal 140 (2008) 264–277

Chemical Engineering Journal

www.elsevier.com/locate/cej

A new solution technique for fluid–solid reactions

A. Shiravani *, E. Jamshidi, H. Ale Ebrahim

Chemical Engineering Department, Petrochemical Center of Excellence, Amir Kabir University, Tehran 15875-4413, Iran

Received 21 March 2007; received in revised form 27 August 2007; accepted 17 September 2007

Abstract

Fluid–solid reactions are very important in the chemical and metallurgical process industries. Several models described these reactions such as volume reaction model, grain model, random pore model and nucleation model. These models give two nonlinear-coupled partial differential equations (CPDE). When the fluid concentration is high (for example in liquid–solid reactions), the fluid mass balance must be written as an unsteady equation. There is not any analytical or approximate solution for these equations, due to its complex CPDE. In this work, a new solution technique (quantized method) has been applied to these unsteady state CPDE. The results of this method (conversion–time profiles) have been compared with some existing numerical solutions with a good accuracy. Therefore, this method can be used for rapid estimation of kinetic parameters from experimental data.

Keywords: Fluid–solid reactions; Mathematical modeling; New solution technique

1. Introduction

Fluid–solid reactions exit in many chemical and metallurgical industries. Some examples for such reactions are reduction of metallic oxides [1–3], roasting of metal sulfides [4], adsorption of acid gases [5,6], catalyst regeneration [7], phosphoric acid production [8], leaching processes [9] and active carbon preparation [10].

Reaction engineering of these processes is based on a series of mathematical modeling [11,12]. These models for a porous solid pellet consist of volume reaction model [13–15], the grain model [16–21], random pore model [22–24] and nucleation model [25,26]. The above-mentioned models give a set of coupled partial differential equations (CPDE). In the liquid reactions or high-pressure gas–solid reactions, the fluid conservation must be considered as an unsteady equation. Therefore, the unsteady CPDE are very tedious and must be solved numerically. There is not any analytical or approximate solution for these complex CPDE. In this work, the unsteady CPDE of the various models have been solved by an incremental analytical (or numerical–analytical) solution called as quantized method. The quantized method has been applied to the gas–solid reaction models (quasi-steady state equations) successfully in the previous papers [27–30]. In the present work, the results of this method have been compared with some existing numerical solutions for the unsteady state case with a good agreement. Therefore, the ability of this method in the unsteady state problems is also verified.

2. Mathematical modeling

Consider the following fluid–solid reaction:

$$A(f) + \upsilon_B B(s) \rightarrow C(f) + \upsilon_D D(s) \quad (1)$$

The following assumptions are applied for the porous pellets:

* Corresponding author.
E-mail address: ashiravani@gmail.com (A. Shiravani).

1385-8947/$ – see front matter © 2007 Elsevier B.V. All rights reserved.
doi:10.1016/j.cej.2007.09.024

Nomenclature

$a = C_A/C_{Ab}$ dimensionless gas concentration
$b = C_B/C_{B0}$ dimensionless solid concentration
C_A gas concentration in the pellet
C_{Ab} bulk gas concentration
C_B solid concentration
C_{B0} initial solid concentration
D_e effective diffusivity in the porous pellet
D_{e0} initial effective diffusivity
D_p diffusion coefficient in the product layer
F_g shape factor of the grains
F_p shape factor of the pellet
i position index
j time index
k_s surface rate constant
k_v volumetric rate constant
M modified Thiele modulus
M_B molecular weight of solid reactant
M_D molecular weight of solid product
n reaction order with respect to solid
r position of each point in the pellet
r_g outlet radius of the grains
r_{g0} initial grain radius
r_{gc} radius of unreacted core in the grains
$r^* = r_{gc}/r_{g0}$ dimensionless unreacted core radius in the grains
$r^{**} = r_g/r_{g0}$ dimensionless outlet grain radius
R pellet characterization length
S_0 reaction surface per unit volume
t time
X solid conversion
$y = r/R$ dimensionless position in the pellet
Z volume change parameter

Greek letters
$\beta = 2k_s(1-\varepsilon_0)/\upsilon_B D_p S_0$ product layer resistance in the random pore model
δ dimensionless effective gas diffusivity
ε pellet porosity
ε_0 initial pellet porosity
ε_D porosity of the product layer
$\theta_g = \upsilon_B k_s C_{Ab} M_B t/(\rho_B r_{g0})$ dimensionless time in the grain models
$\theta_n = \upsilon_B k_v C_{Ab} t$ dimensionless time in the nucleation model
$\theta_r = k_s S_0 C_{Ab} t/(C_{B0}(1-\varepsilon_0))$ dimensionless time in the random pore model
$\theta_v = \upsilon_B k_v C_{Ab} C_{B0}^{n-1} t$ dimensionless time in the volume reaction model
ν_B stoichiometric coefficient of solid reactant
ν_D stoichiometric coefficient of solid product
ρ_B density of the solid reactant
ρ_D density of the solid product
$\sigma = R\sqrt{F_g k_s(1-\varepsilon_0)/(D_{e0} r_{g0})}$ Thiele modulus of the grain models
$\sigma_g = \sqrt{k_s r_{g0}/(2F_g D_p)}$ Thiele modulus of the grains
$\hat{\sigma}_N = R\sqrt{k_v \rho_B(1-\varepsilon)/(2F_p D_e M_B)}$ Thiele modulus of the nucleation model
$\phi_r = R\sqrt{k_s S_0/(\upsilon_B D_{e0})}$ Thiele modulus of the random pore model
$\phi_v = R\sqrt{k_v C_{B0}^n/D_{e0}}$ Thiele modulus of the volume reaction model
$\psi = \varepsilon C_{Ab}/((1-\varepsilon)C_{B0})$ accumulation parameter
Ψ random pore model parameter

(1) The reaction is irreversible and first-order with respect to the fluid concentration. The most of power law or Langmuir–Hinshelwood kinetics could also be approximated by first-order reactions [11].
(2) The pseudo-steady state approximation (for gas–solid reactions) is not valid for liquid–solid reactions. Therefore the fluid mass balance is considered as an unsteady state equation.
(3) External mass transfer resistance is negligible for relatively small pellets and at the moderate temperatures.
(4) Bulk fluid concentration is constant at the single pellet systems.
(5) The overall pellet size is constant. In the nonporous pellets, the solid volume change during the reaction causes the pellet size to change. But in the porous pellets, this effect causes the porosity to change and pellet size usually remains constant.
(6) The bulk flow effect is negligible and system is assumed as equimolar counter-diffusion.
(7) The system is isothermal for relatively low heat of reactions.

Now the differential equations of the various models for the porous pellets at unsteady state case are presented.

2.1. Volume reaction models

The fluid and solid concentration equations with boundary and initial conditions for this model are as follows [31]:

$$\psi\phi_{\mathrm{v}}^2\frac{\partial a}{\partial\theta_{\mathrm{v}}} = \frac{\partial^2 a}{\partial y^2} + \frac{F_{\mathrm{p}}-1}{y}\frac{\partial a}{\partial y} - \phi_{\mathrm{v}}^2 a b^n \tag{2}$$

$$\frac{\partial b}{\partial\theta_{\mathrm{v}}} = -ab^n \tag{3}$$

$$y = 0, \quad \frac{\partial a}{\partial y} = 0 \tag{4}$$

$$y = 1, \quad a = 1 \tag{5}$$

$$\theta_{\mathrm{v}} = 0, \quad a = 0,\ b = 1 \tag{6}$$

In the above equations, n is the reaction order with respect to the solid and $n = 1$ and 1/2 for first and half orders, respectively. Moreover, $F_{\mathrm{p}} = 1$ and 3 for slab and sphere pellets geometry. In the half-order reaction, the reaction completion time (θ_{c}) is finite and after θ_{c}, two diffusion and diffusion-reaction zones appear. However in the first-order reaction, θ_{c} is infinite and only diffusion-reaction zone exists. By solving the above equations, pellet conversion can be computed as follows:

$$X(\theta) = 1 - F_{\mathrm{p}}\int_0^1 y^{F_{\mathrm{p}}-1} b\,\mathrm{d}y \tag{7}$$

2.2. Grain models

The differential equations for the simple grain model are as follows [16]:

$$\psi\sigma^2\frac{\partial a}{\partial\theta_{\mathrm{g}}} = \frac{\partial^2 a}{\partial y^2} + \frac{F_{\mathrm{p}}-1}{y}\frac{\partial a}{\partial y} - \sigma^2 r^{*F_{\mathrm{g}}-1} a \tag{8}$$

$$\frac{\partial r^*}{\partial\theta_{\mathrm{g}}} = -a \tag{9}$$

In the above equations, r^* is the dimensionless radius of unreacted core in each grain and F_{g} is the grain shape factor ($r^* = 1$ at time zero). The pellet consists of several fine grains, and two stage reactions (with moving boundary in the second stage between diffusion and diffusion-reaction zones) exist.

The following equations are for the grain model with the product layer resistance (spherical pellet and grains) [18]:

$$\psi\sigma^2\frac{\partial a}{\partial\theta_{\mathrm{g}}} = \frac{\partial^2 a}{\partial y^2} + \frac{2}{y}\frac{\partial a}{\partial y} - \frac{\sigma^2 r^{*^2} a}{1 + 6\sigma_{\mathrm{g}}^2(r^* - r^{*^2})} \tag{10}$$

$$\frac{\partial r^*}{\partial\theta_{\mathrm{g}}} = -\frac{a}{1 + 6\sigma_{\mathrm{g}}^2(r^* - r^{*^2})} \tag{11}$$

In this case, the product layer resistance around each grain is also considered.

Finally for the modified grain model (with spherical pellet and grains), the governing equations are as follows [20]:

$$\psi\sigma^2\frac{\partial a}{\partial\theta_g}=\frac{1}{y^2}\frac{\partial}{\partial y}\left(\delta y^2\frac{\partial a}{\partial y}\right)-\frac{\sigma^2 r^{*^2}a}{1+6\sigma_g^2(r^*-(r^{*^2}/r^{**}))} \tag{12}$$

$$\frac{\partial r^*}{\partial\theta_g}=-\frac{a}{1+6\sigma_g^2(r^*-(r^{*^2}/r^{**}))} \tag{13}$$

$$r^{**}=[Z+(1-Z)\,r^{*^3}]^{1/3} \tag{14}$$

$$Z=\frac{\upsilon_D\rho_B M_D}{\upsilon_B\rho_D M_B(1-\varepsilon_D)} \tag{15}$$

$$\frac{1-\varepsilon}{1-\varepsilon_0}=r^{**^3} \tag{16}$$

$$\delta(r^*)=\frac{D_e}{D_{e0}}=\left(\frac{\varepsilon}{\varepsilon_0}\right)^2=\left[1-\frac{1-\varepsilon_0}{\varepsilon_0}(Z-1)(1-r^{*^3})\right]^2 \tag{17}$$

In this modified grain model, the structural changes due to the reaction are considered. This means, for $Z<1$ the grains shrink, and for $Z>1$ the grains expand during the reaction. In the high Z values (for example for $CaO+SO_2$ reaction with $Z=3$), the pore mouth blocking and incomplete conversion may occur. In the grain models, solid conversion is computed as follows:

$$X(\theta)=1-F_p\int_0^1 y^{F_p-1}r^{*^{F_g}}\,dy \tag{18}$$

2.3. Random pore model

Random pore model assumes that the porous pellet consist of a series of cylindrical pores with a size distribution. This pore size distribution determines the parameter Ψ in this model. Moreover, the structural changes (due to various molar volumes of solid reactant and solid product), and product layer resistance are also considered. The differential equations of unsteady state random pore model for a spherical pellet are as follows [24]:

$$\psi\phi_r^2\frac{\partial a}{\partial\theta_r}=\frac{1}{y^2}\frac{\partial}{\partial y}\left(\delta y^2\frac{\partial a}{\partial y}\right)-\frac{\phi_r^2 ab\sqrt{1-\Psi\ln(b)}}{1+(\beta Z/\Psi)\left[\sqrt{1-\Psi\ln(b)}-1\right]} \tag{19}$$

$$\frac{\partial b}{\partial\theta_r}=-\frac{ab\sqrt{1-\Psi\ln(b)}}{1+(\beta Z/\Psi)\left[\sqrt{1-\Psi\ln(b)}-1\right]} \tag{20}$$

2.4. Nucleation model

The nucleation phenomenon usually appears in some of the reactions such as metallic oxides reduction. In this case, the conversion–time behavior consists of three stages (sigmoidal curve). The differential equations for the nucleation model ($n=3$) and for a spherical pellet are as follows [26]:

$$\psi\hat{\sigma}_N^2\frac{\partial a}{\partial\theta_n}=\frac{\partial^2 a}{\partial y^2}+\frac{2}{y}\frac{\partial a}{\partial y}-18\hat{\sigma}_N^2 b[-\ln(b)]^{2/3}a \tag{21}$$

$$\frac{\partial b}{\partial\theta_n}=-3b[-\ln(b)]^{2/3}a \tag{22}$$

3. Solution technique

The above complex-coupled partial differential equations must be solved numerically. In the numerical solution, these partial differential equations are changed in stepwise elements. This method usually leads to a large set of related algebraic equations. These equations must be solved simultaneously with large computational time.

In this quantized or incremental method, just opposite of the numerical solution, the independency between parameters is used. This means that $a(j, i)$ is related to $b(j, i)$ but is independent of $b(j-1, i)$ or $b(j, i-1)$, where j and i are the time and position indexes, respectively. In other words, the variables a, b, θ and y are related to each other on their state of (j, i). Therefore, they are independent for other states such as $(j-1, i)$ or $(j, i-1)$. If one uses $b(j-1, i)$ instead of $b(j, i)$ for example in Eq. (2) as an approximation,

some errors of computation are expected. This means that b is treated as a constant between two small time increments in Eq. (2). In the previous papers, it has been shown that this error is small for the gas–solid reactions with the pseudo-steady state assumption [27–30]. In the fluid–solid reactions with unsteady state equations (after this approximation in Eq. (2)), it is possible to solve Eq. (2) analytically for obtaining a or fluid concentration profile in the pellet. Then a is inserted to Eq. (3) and one can compute b or solid concentration profile by integration of this equation. Therefore by this quantized method, the unsteady-coupled partial differential equations can be solved analytically for small time increments. This procedure is continued until the final required time. Recently, this quantized method has been used for decoupling and solving of the governing equations of various gasification models successfully [32].

Now the final solution equations for the various fluid–solid reaction models (with unsteady state conservation equation) by this new method are presented.

3.1. Volume reaction models

The solution for the first-order volume reaction model of a slab pellet is as follows:

$$M = \phi_{\mathrm{v}} b(j-1,i)^{1/2} \tag{23}$$

$$a = \frac{\cosh(My)}{\cosh(M)} + \sum_{k=1}^{\infty} \frac{k\pi(-1)^k \cos(k\pi y/2)}{M^2 + (k^2\pi^2/4)} \exp\left[-\frac{(M^2 + (k^2\pi^2/4))\theta}{\psi\phi_{\mathrm{v}}^2}\right] \tag{24}$$

$$b = \exp\left[2 - \frac{\cosh(My)}{\cosh(M)}\theta - \sum_{k=1}^{\infty} \frac{k\pi(-1)^k \cos(k\pi y/2)}{M^2 + (k^2\pi^2/4)} \frac{\psi\phi_u^2}{M^2 + (k^2\pi^2/4)} \left(1 - \exp\left[-\frac{(M^2 + (k^2\pi^2/4))\theta}{\psi\phi_{\mathrm{v}}^2}\right]\right)\right] \tag{25}$$

First-order volume reaction model for a spherical pellet is solved as follows:

$$a = \frac{\sinh(My)}{y\sinh(M)} + \sum_{k=1}^{\infty} \frac{2k\pi(-1)^k \sin(k\pi y)}{(M^2 + k^2\pi^2)y} \exp\left[-\frac{(M^2 + k^2\pi^2)\theta}{\psi\phi_{\mathrm{v}}^2}\right] \tag{26}$$

$$b = \exp\left[2 - \frac{\sinh(My)}{y\sinh(M)}\theta - \sum_{k=1}^{\infty} \frac{2k\pi(-1)^k \sin(k\pi y)}{(M^2 + k^2\pi^2)y} \frac{\psi\phi_{\mathrm{v}}^2}{M^2 + k^2\pi^2} \left(1 - \exp\left[-\frac{(M^2 + k^2\pi^2)\theta}{\psi\phi_{\mathrm{v}}^2}\right]\right)\right] \tag{27}$$

This means that from initial condition (6) and Eq. (23), the modified Thiele modulus (M) can be computed at each position and for the first time increment. Then by Eq. (24) or (26) the dimensionless fluid concentration in each position and for the first time increment is computed. Also in Eq. (25) or (27) the dimensionless solid concentration in each position and for the first time increment is determined. Now these solid concentrations are inserted to Eq. (23) for computing M at each position and for the second time increment. This procedure is continued until the final dimensionless time. Finally, the conversion–time profile is determined by Eq. (7).

In the half-order volume reaction model with slab geometry, the following solution is obtained for the first stage:

$$M = \phi_{\mathrm{v}} b(j-1,i)^{1/4} \tag{28}$$

$$a = \frac{\cosh(My)}{\cosh(M)} + \sum_{k=1}^{\infty} \frac{k\pi(-1)^k \cos(k\pi y/2)}{M^2 + (k^2\pi^2/4)} \exp\left[-\frac{(M^2 + (k^2\pi^2/4))\theta}{\psi\phi_{\mathrm{v}}^2}\right] \tag{29}$$

$$b = \left[1 - \frac{\cosh(My)}{\cosh(M)}\frac{\theta}{2} - \sum_{k=1}^{\infty} \frac{(k\pi/2)(-1)^k \cos(k\pi y/2)}{M^2 + (k^2\pi^2/4)} \left(\frac{\psi\phi_{\mathrm{v}}^2}{M^2 + (k^2\pi^2/4)}\right) \left(1 - \exp\left[-\frac{(M^2 + (k^2\pi^2/4))\theta}{\psi\phi_{\mathrm{v}}^2}\right]\right)\right]^2 \tag{30}$$

For the second stage ($\theta > \theta_{\mathrm{c}} = 2$) the solution is as follows:

$$\theta = 2 + M^2(1 - y_{\mathrm{m}})^2 + 2M(1 - y_{\mathrm{m}})\tanh(My_{\mathrm{m}}) \tag{31}$$

$$b = \left[1 - \frac{\cosh(My)}{\cosh(My_{\mathrm{m}})} - \sum_{k=1}^{\infty} \frac{(k\pi/2y_{\mathrm{m}})(-1)^k \cos(k\pi y/2y_{\mathrm{m}})}{M^2 + (k^2\pi^2/4y_{\mathrm{m}}^2)} \frac{\psi\phi_{\mathrm{v}}^2}{M^2 + (k^2\pi^2/4y_{\mathrm{m}}^2)} \left(1 - \exp\left[-\left(M^2 + \frac{k^2\pi^2}{4y_{\mathrm{m}}^2}\right)\frac{\theta_{\mathrm{c}}}{\psi\phi_{\mathrm{v}}^2}\right]\right)\right]^2 \tag{32}$$

Finally for the spherical geometry half-order volume reaction model, the following solution is obtained for the first and second stages, respectively:

$$a = \frac{\sinh(My)}{y\sinh(M)} + \sum_{k=1}^{\infty} \frac{2k\pi(-1)^k \sin(k\pi y)}{(M^2 + k^2\pi^2)y} \exp\left[-\frac{(M^2 + k^2\pi^2)\theta}{\psi\phi_v^2}\right] \tag{33}$$

$$b = \left[1 - \frac{\sinh(My)}{y\sinh(M)}\frac{\theta}{2} - \sum_{k=1}^{\infty} \frac{k\pi(-1)^k \sin(k\pi y)}{(M^2 + k^2\pi^2)y} \frac{\psi\phi_v^2}{M^2 + k^2\pi^2}\left(1 - \exp\left[-\frac{(M^2 + k^2\pi^2)\theta}{\psi\phi_v^2}\right]\right)\right]^2 \tag{34}$$

$$\theta = 2 + \frac{M^2}{3}(1 - y_m)^2(1 + 2y_m) + 2(1 - y_m)[My_m \coth(My_m) - 1] \tag{35}$$

$$b = \left[1 - \frac{y_m \sinh(My)}{y\sinh(My_m)} - \sum_{k=1}^{\infty} \frac{(k\pi/y_m)(-1)^k \sin(k\pi y/y_m)}{(M^2 + (k^2\pi^2/y_m^2))y} \frac{\psi\phi_v^2}{M^2 + (k^2\pi^2/y_m^2)}\left(1 - \exp\left[-\left(M^2 + \frac{k^2\pi^2}{y_m^2}\right)\frac{\theta_c}{\psi\phi_v^2}\right]\right)\right]^2 \tag{36}$$

3.2. Grain models

Application of this new solution technique to the unsteady differential equations of the simple grain model (slab pellet) leads to the following equations:

$$M = \sigma\sqrt{r^{*^{Fg-1}}} \tag{37}$$

$$a = \frac{\cosh(My)}{\cosh(M)} + \sum_{k=1}^{\infty} \frac{k\pi(-1)^k \cos(k\pi y/2)}{M^2 + (k^2\pi^2/4)} \exp\left[-\frac{(M^2 + (k^2\pi^2/4))\theta}{\psi\sigma^2}\right] \tag{38}$$

$$r^* = 1 - \frac{\cosh(My)}{\cosh(M)}\theta - \sum_{k=1}^{\infty} \frac{k\pi(-1)^k \cos(k\pi y/2)}{M^2 + (k^2\pi^2/4)}\left(\frac{\psi\sigma^2}{M^2 + (k^2\pi^2/4)}\right)\left(1 - \exp\left[-\frac{(M^2 + (k^2\pi^2/4))\theta}{\psi\sigma^2}\right]\right) \tag{39}$$

In the second stage ($\theta > \theta_c = 1$), the following solution is obtained:

$$\theta = 1 + \frac{M^2}{2}(1 - y_m)^2 + M(1 - y_m)\tanh(My_m) \tag{40}$$

$$r^* = 1 - \frac{\cosh(My)}{\cosh(My_m)} - \sum_{k=1}^{\infty} \frac{(k\pi/y_m)(-1)^k \cos(k\pi y/2y_m)}{M^2 + (k^2\pi^2/4y_m^2)}\left(\frac{\psi\sigma^2}{M^2 + (k^2\pi^2/4y_m^2)}\right)\left(1 - \exp\left[-\left(M^2 + \frac{k^2\pi^2}{4y_m^2}\right)\frac{\theta_c}{\psi\sigma^2}\right]\right) \tag{41}$$

For the spherical geometry, the following solution is obtained for the first and second stages, respectively:

$$a = \frac{\sinh(My)}{y\sinh(M)} + \sum_{k=1}^{\infty} \frac{2k\pi(-1)^k \sin(k\pi y)}{(M^2 + k^2\pi^2)y} \exp\left[-\frac{(M^2 + k^2\pi^2)\theta}{\psi\sigma^2}\right] \tag{42}$$

$$r^* = 1 - \frac{\sinh(My)}{y\sinh(M)}\theta - \sum_{k=1}^{\infty} \frac{2k\pi(-1)^k \sin(k\pi y)}{(M^2 + k^2\pi^2)y} \frac{\psi\sigma^2}{M^2 + k^2\pi^2}\left(1 - \exp\left[-\frac{(M^2 + k^2\pi^2)\theta}{\psi\sigma^2}\right]\right) \tag{43}$$

$$\theta = 1 + \frac{M^2}{6}(1 - y_m)^2(1 + 2y_m) + (1 - y_m)[My_m \coth(My_m) - 1] \tag{44}$$

$$r^* = 1 - \frac{\sinh(My)}{y\sinh(My_m)}\theta - \sum_{k=1}^{\infty} \frac{(2k\pi/y_m)(-1)^k \sin(k\pi y/y_m)}{(M^2 + (k^2\pi^2/y_m^2))y} \frac{\psi\sigma^2}{M^2 + (k^2\pi^2/y_m^2)}\left(1 - \exp\left[-\left(M^2 + \frac{k^2\pi^2}{y_m^2}\right)\frac{\theta_c}{\psi\sigma^2}\right]\right) \tag{45}$$

In the grain model with product layer resistance, the solution in the first stage for a spherical pellet and spherical grains is as follows:

$$M = \sigma\sqrt{\frac{r^{*^2}}{1 + 6\sigma_g^2(r^* - r^{*^2})}} \tag{46}$$

$$a = \frac{\sinh(My)}{y\sinh(M)} + \sum_{k=1}^{\infty} \frac{2k\pi(-1)^k \sin(k\pi y)}{(M^2 + k^2\pi^2)y} \exp\left[-\frac{(M^2 + k^2\pi^2)\theta}{\psi\sigma^2}\right] \tag{47}$$

$$r^* + 3\sigma_g^2 r^{*^2} - 2\sigma_g^2 r^{*^3} = 1 + \sigma_g^2 - \frac{\sinh(My)}{y\sinh(M)}\theta - \sum_{k=1}^{\infty} \frac{2k\pi(-1)^k \sin(k\pi y)}{(M^2 + k^2\pi^2)y} \frac{\psi\sigma^2}{M^2 + k^2\pi^2} \left(1 - \exp\left[\frac{-(M^2 + k^2\pi^2)\theta}{\psi\sigma^2}\right]\right) \tag{48}$$

In the second stage ($\theta > \theta_c = 1 + \sigma_g^2$), the following solution is obtained:

$$\frac{\theta}{1 + \sigma_g^2} = 1 + \frac{M^2}{6}(1 - y_m)^2(1 + 2y_m) + (1 - y_m)[My_m \coth(My_m) - 1] \tag{49}$$

$$r^* + 3\sigma_g^2 r^{*^2} - 2\sigma_g^2 r^{*^3} = 1 + \sigma_g^2 - \frac{y_m \sinh(My)}{y\sinh(My_m)}\theta_c - \sum_{k=1}^{\infty} \frac{(2k\pi/y_m)(-1)^k \sin(k\pi y/y_m)}{(M^2 + (k^2\pi^2/y_m^2))y} \frac{\psi\sigma^2}{M^2 + (k^2\pi^2/y_m^2)} \times \left(1 - \exp\left[-\left(M^2 + \frac{k^2\pi^2}{y_m^2}\right)\frac{\theta_c}{\psi\sigma^2}\right]\right) \tag{50}$$

In the modified grain model, the solution for a spherical pellet and spherical grains in the first stage is as follows:

$$M = \sigma\sqrt{\frac{r^{*^2}}{[1 + 6\sigma_g^2(r^* - (r^{*^2}/r^{**}))]\delta(r^*)}} \tag{51}$$

$$a = \frac{\sinh(My)}{y\sinh(M)} + \sum_{k=1}^{\infty} \frac{2k\pi(-1)^k \sin(k\pi y)}{(M^2 + k^2\pi^2)y} \exp\left[-\frac{(M^2 + k^2\pi^2)\theta}{\psi\sigma^2/\delta}\right] \tag{52}$$

$$r^* + 3\sigma_g^2 r^{*^2} + \frac{3\sigma_g^2}{Z-1}[Z + (1 - Z)r^{*^3}]^{2/3} = 1 + \left(3 + \frac{3}{Z-1}\right)\sigma_g^2 - \frac{\sinh(My)}{y\sinh(M)}\theta - \sum_{k=1}^{\infty} \frac{2k\pi(-1)^k \sin(k\pi y)}{(M^2 + k^2\pi^2)y} \frac{\psi\sigma^2/\delta}{M^2 + k^2\pi^2} \left(1 - \exp\left[-\frac{(M^2 + k^2\pi^2)\theta}{\psi\sigma^2/\delta}\right]\right) \tag{53}$$

In the second stage ($\theta > \theta_c = 1 + 3\sigma_g^2 + (3\sigma_g^2/(Z-1))(1 - Z^{2/3})$), the following solution is obtained:

$$\frac{\theta}{\theta_c} = 1 + \frac{M^2}{6}(1 - y_m)^2(1 + 2y_m) + (1 - y_m)[My_m \coth(My_m) - 1] \tag{54}$$

$$r^* + 3\sigma_g^2 r^{*^2} + \frac{3\sigma_g^2}{Z-1}[Z + (1 - Z)r^{*^3}]^{2/3} = 1 + \left(3 + \frac{3}{Z-1}\right)\sigma_g^2 - \frac{y_m \sinh(My)}{y\sinh(My_m)}\theta_c - \sum_{k=1}^{\infty} \frac{(2k\pi/y_m)(-1)^k \sin(k\pi y/y_m)}{(M^2 + (k^2\pi^2/y_m^2))y} \frac{\psi\sigma^2/\delta}{M^2 + (k^2\pi^2/y_m^2)} \times \left(1 - \exp\left[-\left(M^2 + \frac{k^2\pi^2}{y_m^2}\right)\frac{\theta_c}{(\psi\sigma^2/\delta)}\right]\right) \tag{55}$$

3.3. Random pore model

The solution for unsteady state random pore model for a spherical pellet and negligible product layer resistance is as follows:

$$M = \phi_r\sqrt{b\sqrt{1 - \Psi\ln(b)}} \tag{56}$$

$$a = \frac{\sinh(My)}{y\sinh(M)} + \sum_{k=1}^{\infty} \frac{2k\pi(-1)^k \sin(k\pi y)}{(M^2 + k^2\pi^2)y} \exp\left[-\frac{(M^2 + k^2\pi^2)\theta}{\psi\phi_r^2}\right] \tag{57}$$

$$\Psi \ln(b) = 1 - \left\{1 + \frac{\Psi}{2}\left[\frac{\sinh(My)}{y\sinh(M)}\theta + \sum_{k=1}^{\infty}\frac{2k\pi(-1)^k\sin(k\pi y)}{(M^2+k^2\pi^2)y}\frac{\psi\phi_r^2}{M^2+k^2\pi^2}\left(1-\exp\left[-\frac{(M^2+k^2\pi^2)\theta}{\psi\phi_r^2}\right]\right)\right]\right\}^2 \quad (58)$$

3.4. Nucleation model

The solution for the unsteady nucleation model with $n=3$ and for a spherical pellet is as follows:

$$M = \hat{\sigma}_N\sqrt{18b[-\ln(b)]^{2/3}} \quad (59)$$

$$a = \frac{\sinh(My)}{y\sinh(M)} + \sum_{k=1}^{\infty}\frac{2k\pi(-1)^k\sin(k\pi y)}{(M^2+k^2\pi^2)y}\exp\left[\frac{-(M^2+k^2\pi^2)\theta}{\psi\hat{\sigma}_N^2}\right] \quad (60)$$

$$b = \exp\left[-\left[\frac{\sinh(My)}{y\sinh(M)}\theta + \sum_{k=1}^{\infty}\frac{2k\pi(-1)^k\sin(k\pi y)}{(M^2+k^2\pi^2)y}\frac{\psi\hat{\sigma}_N^2}{M^2+k^2\pi^2}\left(1-\exp\left[-\frac{(M^2+k^2\pi^2)\theta}{\psi\hat{\sigma}_N^2}\right]\right)\right]^3\right] \quad (61)$$

4. Comparison of results

The conversion–time profile for the first-order volume reaction model (slab pellet) and $\psi=0.1$ is presented in Fig. 1 and is compared with orthogonal collocation solution of Ref. [31]. The comparison for half-order volume reaction model of the slab pellet with numerical solution of Ref. [15] is presented in Fig. 2. Fig. 3 is the similar comparison with Ref. [15] for the half-order volume reaction model in a sphere pellet. As these figures show, there are a good agreement between the quantized solution and numerical solution especially for low and intermediate Thiele modulus. However at high Thiele modulus or diffusion control regime (with the resulting steep concentration gradients in the pellet) the approximation of using $b(j-1, i)$ instead of $b(j, i)$ in Eq. (2) introduces more errors.

The effect of unsteady state parameter (ψ) in the conversion–time behavior of half-order volume reaction model for a spherical pellet (with $\phi=5$) is presented in Fig. 4. As Fig. 4 shows, for $\psi>0.1$ the pseudo-steady state approximation is not valid and the unsteady state equations must be used.

The conversion–time profiles for the simple grain model with sphere pellet and for spherical and cylindrical grains are presented in Figs. 5 and 6, respectively. The grain model with product layer resistance, and modified grain model (with $Z=1.5$) are presented in Figs. 7 and 8, respectively. The modified grain model behavior for high Z values is presented in Fig. 9, which shows the pore closure and incomplete conversion. The comparison for unsteady state random pore model ($\psi=0.5$) with Ref. [24] is presented in Fig. 10 with a good accuracy. Finally the comparison for the nucleation model ($n=3$) with Ref. [26] is presented in Fig. 11 successfully.

The actual value of the calculations of this work in comparison with the literature data are presented in Tables 1–4 for Figs. 1, 3, 10 and 11, respectively.

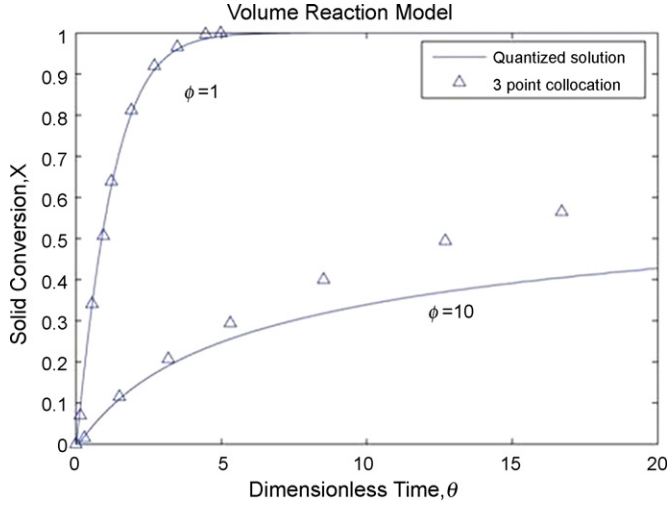

Fig. 1. Comparison of results of this work and orthogonal collocation of Ref. [31] for slab pellets, $\psi=0.1$.

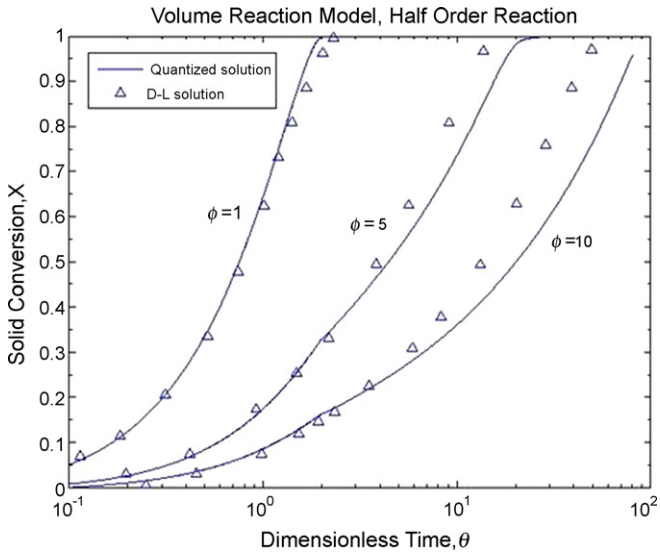

Fig. 2. Comparison for half-order reaction model of the slab pellets with numerical solution of Ref. [15], $\psi = 0.1$.

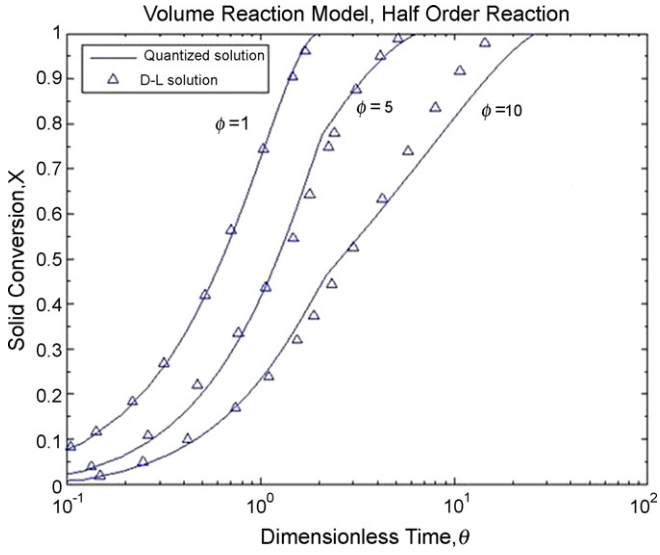

Fig. 3. Comparison for half-order reaction model of the spherical pellets with numerical solution of Ref. [15], $\psi = 0.1$.

Table 1
Comparison of results of this work and orthogonal collocation of Ref. [31] for slab pellets, $\psi = 0.1$

Dimensionless time, θ	Solid conversion, X			
	Quantized solution, $\phi_v = 1$	Three-point collocation, $\phi_v = 1$	Quantized solution, $\phi_v = 10$	Three-point collocation, $\phi_v = 10$
2	0.823	0.826	0.139	0.144
3	0.938	0.933	0.185	0.197
4	0.979	0.982	0.221	0.239
5	0.995	0.999	0.249	0.280
6	0.997	1	0.273	0.315
8	1	1	0.311	0.377
10	1	1	0.339	0.431
12	1	1	0.365	0.474
14	1	1	0.383	0.515
16	1	1	0.399	0.551

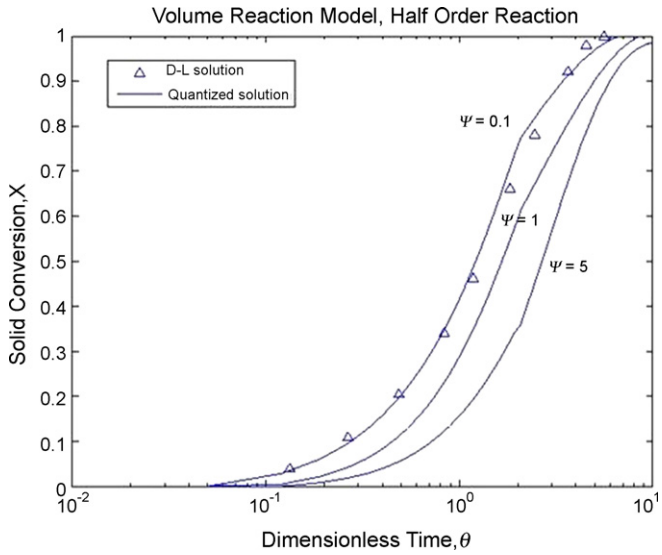

Fig. 4. Effect of unsteady state parameter (ψ) in the conversion–time behavior of half-order volume reaction model for spherical pellet, $\phi = 5$.

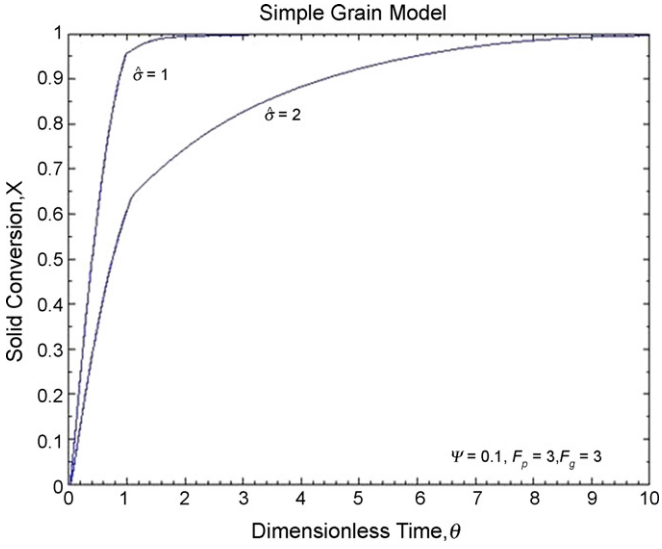

Fig. 5. Conversion–time profiles for the simple grain model with sphere pellets and sphere grains, $\hat{\sigma} = \sigma/\sqrt{2F_{\mathrm{p}}F_{\mathrm{g}}}$.

Table 2
Comparison for half-order reaction model of the spherical pellets with numerical solution of Ref. [15], $\psi = 0.1$

Dimensionless time, θ	Solid conversion, X					
	Quantized solution, $\phi_{\mathrm{v}} = 1$	D–L solution, $\phi_{\mathrm{v}} = 1$	Quantized solution, $\phi_{\mathrm{v}} = 5$	D–L solution, $\phi_{\mathrm{v}} = 5$	Quantized solution, $\phi_{\mathrm{v}} = 10$	D–L solution, $\phi_{\mathrm{v}} = 10$
0.2	0.164	0.174	0.069	0.082	0.031	0.041
0.4	0.331	0.346	0.162	0.187	0.084	0.095
0.6	0.480	0.495	0.251	0.277	0.130	0.146
0.8	0.601	0.628	0.328	0.349	0.184	0.182
1	0.724	0.733	0.423	0.423	0.241	0.223
2	0.999	1	0.769	0.697	0.436	0.392
4	1	1	0.936	0.941	0.600	0.621
6	1	1	1	1	0.692	0.751
8	1	1	1	1	0.756	0.833
10	1	1	1	1	0.815	0.908
20	1	1	1	1	0.962	1

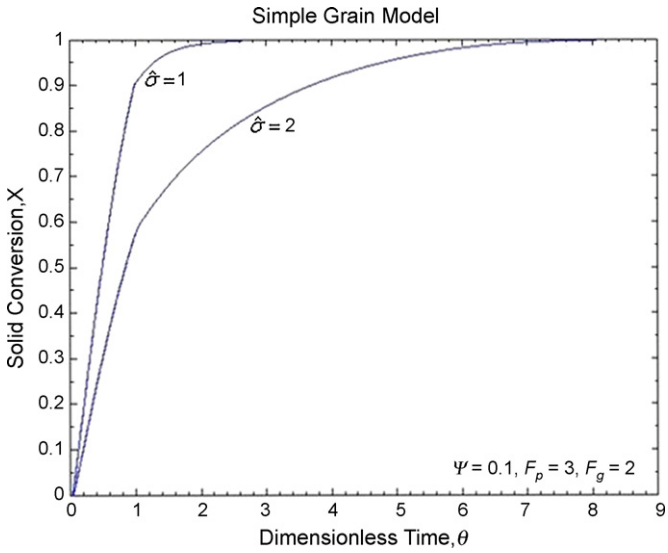

Fig. 6. Conversion–time profiles for the simple grain model with sphere pellet and cylindrical grains, $\hat{\sigma} = \sigma/\sqrt{2F_{\mathrm{p}}F_{\mathrm{g}}}$.

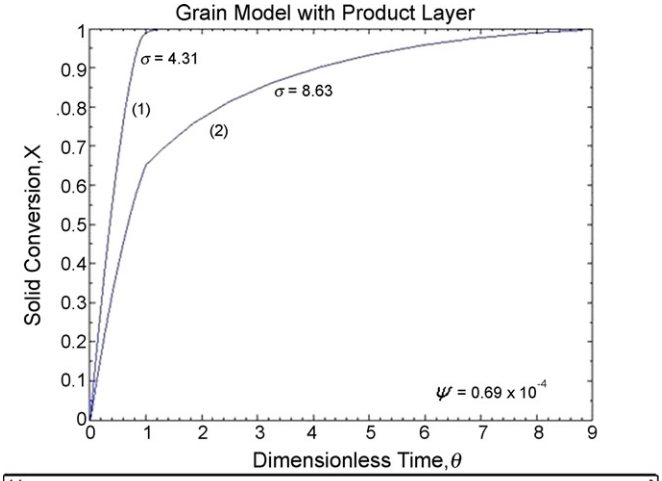

Fig. 7. Conversion–time profiles for grain model with product layer resistance for reduction of barium sulphate with methane gas.

Table 3
Comparison for unsteady state random pore model ($\psi = 0.5$) with Ref. [21]

Dimensionless time, θ	Solid conversion, X			
	Quantized solution	Numerical solution	Composite solution	PSS solution
0.5	0.245	0.248	0.247	0.306
1.0	0.488	0.483	0.475	0.552
1.5	0.698	0.673	0.663	0.734
2.0	0.859	0.814	0.807	0.860
2.5	0.956	0.905	0.901	0.934
3.0	0.976	0.941	0.939	0.963

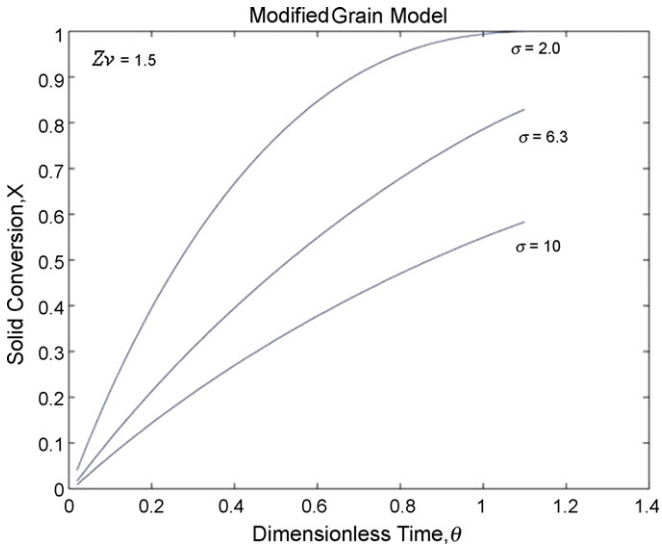

Fig. 8. Conversion–time profiles for modified grain model with $Z = 1.5$, $\psi = 0.1$.

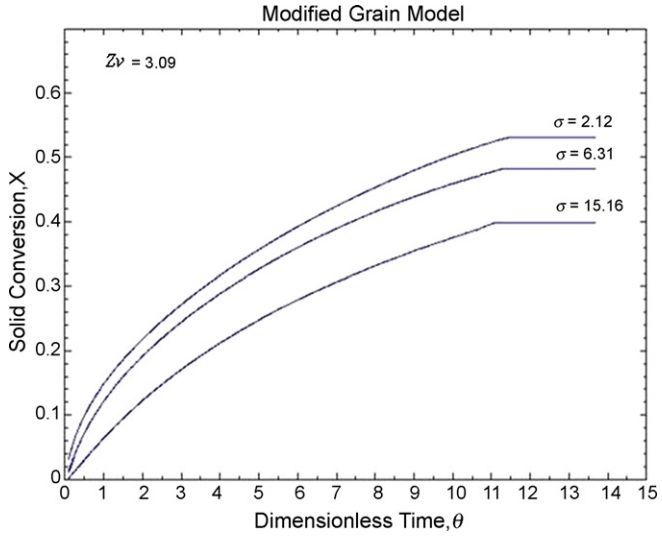

Fig. 9. Modified grain model behavior for high Z values ($CaO + SO_2$ system), $\psi = 0.1$.

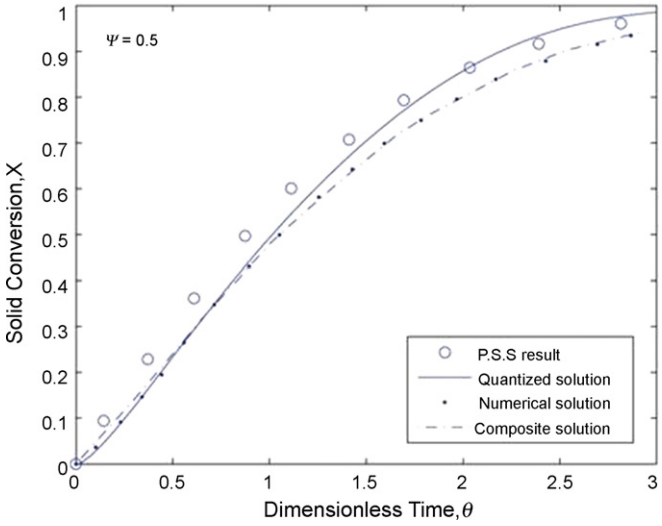

Fig. 10. Comparison for unsteady state random pore model ($\psi = 0.5$) with Ref. [21].

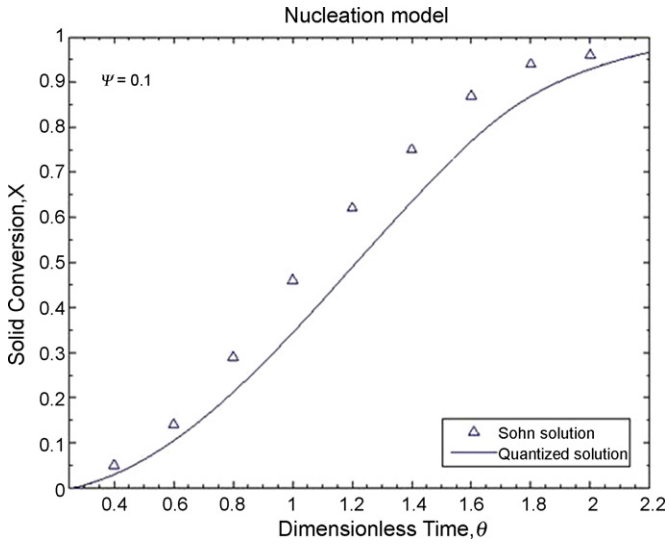

Fig. 11. Comparison for the nucleation model ($n = 3$) with Ref. [26], $\psi = 0.1$.

Table 4
Comparison for the nucleation model ($n = 3$) with Ref. [26], $\psi = 0.1$

Dimensionless time, θ	Solid conversion, X	
	Quantized solution	Sohn solution
0.4	0.031	0.051
0.6	0.105	0.143
0.8	0.213	0.292
1.0	0.346	0.459
1.2	0.492	0.621
1.4	0.636	0.752
1.6	0.772	0.872
1.8	0.869	0.936
2.0	0.931	0.962

5. Conclusion

In this paper the fluid–solid reactions with their unsteady state differential equations were considered. There is not any analytical or approximate solution for these equations due to the complex-coupled partial differential equations. In this work, a new solution technique (quantized method) has been used for the fluid–solid reactions. Comparison of the results of this work with some existing numerical solutions showed good agreements. Therefore, this method can be applied for the rapid estimation of model parameters from the experimental data with reduced computational effort.

References

[1] J. Szekely, C.I. Lin, H.Y. Sohn, A structural model for gas–solid reactions with a moving boundary. V. An experimental study of the reduction of porous nickel-oxide pellets with hydrogen, Chem. Eng. Sci. 28 (1973) 1975–1989.
[2] K.L. Breg, S.E. Olsen, Kinetics of manganese ore reduction by carbon monoxide, Met. Mater. Trans. B 31 (2000) 477–490.
[3] H. Ale Ebrahim, E. Jamshid, Kinetic study and mathematical modeling of the reduction of ZnO–PbO mixtures by methane, Ind. Eng. Chem. Res. 44 (2005) 495–504.
[4] S. Kimura, Oxidation kinetics of polycrystalline zinc sulfide grains, AIChE J. 35 (1989) 339–342.
[5] S. Zarkanitis, S.V. Sotirchos, Pore structure and particle size effect on limestone capacity for SO_2 removal, AIChE J. 35 (1989) 821–830.
[6] E.A. Efthimiadis, S.V. Sotirchos, Reactivity evolution during sulfidation of porous zinc oxide, Chem. Eng. Sci. 48 (1993) 829–843.
[7] P.A. Ramachandran, M.H. Rashid, R. Hughes, A model for coke oxidation from catalyst pellets in the initial burning period, Chem. Eng. Sci. 30 (1975) 1391–1398.
[8] S.I. Abu Eishan, N.M. Abu Jabal, Parametric study on the production of phosphoric acid by dehydrate process, Chem. Eng. J. 81 (2001) 231–250.
[9] D. Dreisinger, Copper leaching from primary sulfides: options for biological and chemical extraction of copper, Hydrometallurgy 83 (2006) 10–20.
[10] G.Q. Lu, D.D. Do, A kinetic study of coal reject derived char activation with CO_2, H_2O and air, Carbon 30 (1992) 21–29.
[11] J. Szekely, J.W. Evans, H.Y. Sohn, Gas–Solid Reactions, Academic Press, New York, 1976.
[12] P.A. Ramachandran, L.K. Doraiswamy, Modeling of noncatalytic gas–solid reactions, AIChE J. 28 (1982) 881–900.

[13] C.Y. Wen, Noncatalytic heterogeneous solid–fluid reaction models, Ind. Eng. Chem. 60 (1968) 34–54.
[14] M. Ishida, C.Y. Wen, Comparison of kinetic and diffusional models for solid–gas reactions, AIChE J. 14 (1968) 311–317.
[15] M.P. Dudukovic, H.S. Lamba, Solution of moving boundary problems for gas–solid noncatalytic reactions by orthogonal collocation, Chem. Eng. Sci. 33 (1978) 303–314.
[16] H.Y. Sohn, J. Szekely, A structural model for gas–solid reactions with a moving boundary. III. A general dimensionless representation of the irreversible reaction between a porous solid and a reactant gas, Chem. Eng. Sci. 27 (1972) 763–778.
[17] J. Szekely, J.W. Evans, Studies in gas–solid reactions. Part I. A structural model for the reaction of porous oxides with a reducing gas, Met. Trans. 2 (1971) 1691–1698.
[18] H.Y. Sohn, J. Szekely, The effect of intragrain diffusion on the reactivity between a porous solid and a gas, Chem. Eng. Sci. 29 (1974) 630–634.
[19] O. Garza-Garza, M.P. Dadukovic, A variable size grain model for gas–solid reactions with structural changes, Chem. Eng. J. 24 (1982) 35–45.
[20] C. Georgakic, C.W. Change, J. Szekely, A changing grain size model for gas–solid reactions, Chem. Eng. Sci. 34 (1979) 1072–1075.
[21] P.V. Ranade, D.P. Harrison, The variable property grain model applied to the zinc oxide–hydrogen sulfide reaction, Chem. Eng. Sci. 36 (1981) 1079–1089.
[22] S.K. Bhatia, D.D. Perlmutter, A random pore model for fluid–solid reactions. I. Isothermal kinetic control, AIChE J. 26 (1980) 379–386.
[23] S.K. Bhatia, D.D. Perlmutter, A random pore model for fluid–solid reaction. II. Diffusion and transport effects, AIChE J. 27 (1981) 247–254.
[24] S.K. Bhatia, On the pseudo-steady state hypothesis for fluid–solid reactions, Chem. Eng. Sci. 40 (1985) 869–872.
[25] E. Ruckenstein, T. Vavanellos, Kinetics of solid phase reactions, AIChE J. 21 (1975) 756–763.
[26] H.Y. Sohn, The law of additive reaction times in fluid–solid reactions, Met. Trans. 9B (1978) 89–96.
[27] E. Jamshidi, H. Ale Ebrahim, A new solution technique of moving boundary problems for gas–solid reactions: application to half-order volume reaction model, Chem. Eng. J. 63 (1996) 79–83.
[28] E. Jamshidi, H. Ale Ebrahim, An incremental analytical solution for gas–solid reactions: application to the grain model, Chem. Eng. Sci. 51 (1996) 4253–4257.
[29] E. Jamshidi, H. Ale Ebrahim, A quantized solution for nucleation model in gas–solid reactions, Chem. Eng. J. 68 (1997) 1–6.
[30] E. Jamshidi, H. Ale Ebrahim, A new solution technique for gas–solid reactions with structural changes, Chem. Eng. Sci. 54 (1999) 859–864.
[31] W.E. King Jr., W.S. Jones, A solution technique for noncatalytic diffusion-reaction models, Chem. Eng. Sci. 34 (1979) 1387–1392.
[32] A.G. Barea, P. Ollero, An approximate method for solving gas–solid non-catalytic reactions, Chem. Eng. Sci. 61 (2006) 3725–3735.